Modelling morphodynamic evolution of river dunes

A.J. Paarlberg, C.M. Dohmen-Janssen & S.J.M.H. Hulscher
University of Twente, Water Engineering & Management, Enschede, The Netherlands

J. van den Berg
University of Twente, Numerical Analysis & Computational Mechanics, Enschede, The Netherlands

A.P.P. Termes
HKV Consultants, Lelystad, The Netherlands

ABSTRACT: River dunes influence the hydraulic roughness and water levels in rivers. Especially during floods the interplay between dunes and the flow field could become significant. Therefore, it is desired to forecast the dimensions of dunes during such extreme and unsteady flood events. At present it is not yet feasible to predict the dimensions of dunes by computing the flow and sediment transport in full detail for operational spatial and temporal scales. In this paper, we present a morphodynamic model that simulates dune development, without computing all details in the flow field. The flow model is based on the 2D-vertical hydrostatic equations, with a constant eddy viscosity over depth. Flow separation and the sediment transport behaviour in the flow separation zone are included in a parameterized way. Results of the morphodynamic model using steady flow conditions, are in general agreement with flume experiments. A next step in the research will be to use forecasted dune dimensions for hydraulic roughness predictions.

1 INTRODUCTION

Water levels during floods in rivers are largely influenced by the flow resistance that results from flow over a dune-covered bed. A flood event itself determines the development of the dunes, leading to a complex interplay of bed formation and flow characteristics.

In current practice, in hydraulic flow models the roughness of the main channel is used as the calibration parameter to match observed water levels. Although the total flow resistance of the river is due to several different sources (e.g. vegetation or groynes), dunes have a large influence on the roughness because of energy dissipation behind steep dunes (e.g. Vanoni and Hwang 1967). During their development, the lee-side of a dune may become so steep that the flow cannot follow the bed surface any longer, forming a flow separation zone. The turbulence (eddies) generated in the flow separation zone slows the flow down. This process is often referred to as form roughness or form drag.

At present, there is still limited knowledge about the effect of dunes on the hydraulic roughness of a river, let alone about their development during floods. In order to understand flow resistance due to dunes, it is necessary to first understand their behaviour. If dune dimensions and their resulting resistance can be predicted as a function of flow conditions and sediment properties, this part of the total flow resistance may be excluded from the calibration of hydraulic models.

Several researchers proposed methods to forecast dune dimensions (e.g. dune length and dune height), based on a range of parameters like flow strength, water depth or sediment size. Part of the proposed methods are empirical (e.g. Julien and Klaassen 1995; Van Rijn 1984), while others are more theoretical (e.g. Kennedy 1969; Onda and Hosoda 2004). All these methods are designed to calculate equilibrium dune dimensions in steady, uniform flow. In that case a unique dune height and dune length exist for each specific combination of flow characteristics and sediment properties.

Observations have shown that changes in flow resistance are out of phase with flood intensity. Maximum dune dimensions occur later than the maximum discharge (e.g. Ten Brinke et al. 1999; Julien et al. 2002). Several researchers tried to include the ob-

served time-lag between dune dimensions and flood intensity in their models to forecast dune dimensions (e.g. Allen 1976; Fredsøe 1979). However, as shown by Wilbers (2004), none of these predictors are able to predict dune dimensions during several floods in the River Rhine in the Netherlands adequately. Wilbers (2004) developed an empirical calculation method to forecast dune development under unsteady flow conditions, based on a method proposed by Allen (1976). This method is applied with success to three sections of the Rhine branches. However, a major drawback is that the method is not generally applicable. For every situation, initial dune dimensions have to be known and data are required to calibrate empirical coefficients. Furthermore, the method gives only limited insight in the physics behind dune development during floods.

To forecast the behaviour of dunes on a physical basis, the flow and sediment transport resulting from that flow has to be predicted. Yoon and Patel (1996) adopted a k-ω turbulence model enabling a detailed computation of the flow in the separation eddy. Results were shown to be in general agreement with the experimental data. Stansby and Zhou (1998) showed that the computation of the flow in the separation zone improved when a non-hydrostatic pressure (instead of hydrostatic) was applied. Nelson et al. (2005) have shown that a large eddy simulation model with non-hydrostatic pressure, in combination with a sediment transport model taking fluctuations of the bed shear stress on turbulent timescales into account, realistically models dune development. Such approaches require modelling all details in the flow field and especially the complex flow in the flow separation zone. A disadvantage of such methods is that they are complicated and require much computational effort. This becomes a problem when the flow calculation has to be done repeatedly for each bottom update.

As a first step towards predicting flow resistance caused by dunes on large spatial and long temporal scales, we propose a morphodynamic model to forecast dune development under steady flow conditions. We aim to develop the most basic morphodynamic model that still describes the most relevant processes to predict dune development.

Paarlberg et al. (2005) have shown that the morphodynamic model of Hulscher (1996), which is originally developed to simulate offshore sandwaves, can also be used to simulate river dunes in unidirectional flows. This morphodynamic model is numerically implemented by Németh et al. (2006) and Van den Berg and Van Damme (2005), of which the latter is used in this research.

The numerical model is based on hydrostatic equations, implying that flow separation cannot be treated explicitly. To keep the model appropriate, we present an approach to include flow separation in a parameterized way. Following the approach of Kroy et al. (2002), the idea is to cut off the flow separation zone from flow computations and only compute the flow above this zone. Paarlberg et al. (2005) showed that the shape of the flow separation can be estimated on the basis of general dune dimensions. Although the predicted shape was in agreement with detailed measurements on turbulent flows over dunes, the parameterization was not tested in a morphodynamic model. Therefore, in this paper, the morphodynamic model is extended with a parameterization of sediment transport behaviour in the flow separation zone, and tested against flume data.

2 MODEL FOR GENTLE DUNES

To simulate dune development, flow and sediment transport due to this flow are modelled. A stationairy version of the code described in Van den Berg and Van Damme (2005) is used for computations. This model is based on earlier models by Hulscher (1996) and Németh and Hulscher (2003). In this section the model equations are discussed. Further, the numerical model is applied to a situation with gentle bed-slopes (i.e. streamlined flow without separation).

2.1 *Steady flow model*

Flow is simulated with the hydrostatic two-dimensional vertical (2DV) shallow water equations. The momentum equation in x-direction and the continuity equation read:

$$u\frac{\partial u}{\partial x} + w\frac{\partial u}{\partial z} = -g\frac{\partial \zeta}{\partial x} + A_v\frac{\partial^2 u}{\partial z^2} + gi \qquad (1)$$

$$\frac{\partial u}{\partial x} + \frac{\partial w}{\partial z} = 0 \qquad (2)$$

The velocities in the x- and z- directions (see Figure 1) are u and w, respectively. The water surface elevation is denoted by ζ, i is the average bottom slope, and g and A_v denote the acceleration due to gravity and the vertical eddy viscosity, respectively.

2.2 *Boundary conditions*

Two boundary conditions are imposed at the water surface ($z = H + \zeta$): (*i*) there is no flow through the surface, and (*ii*) there is no shear stress at the surface:

$$u\frac{\partial \zeta}{\partial x} = w \qquad (3)$$

$$\frac{\partial u}{\partial z} = 0 \qquad (4)$$

The boundary condition at the bed ($z = h$) is that there is no flow through the boundary:

$$u\frac{\partial h}{\partial x} = w \qquad (5)$$

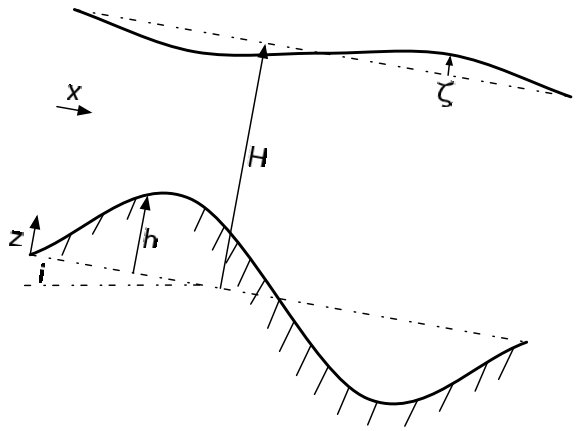

Figure 1. Definitions of H (average height of the water column), $h(x)$ (bottom disturbance) and $\zeta(x,t)$ (surface elevation).

As a basic turbulence closure, a constant eddy viscosity is used. In combination with the fundamental property of boundary layers, the no-slip boundary condition leads to an over-prediction of the shear stress at the bed. Soulsby (1990) has made a comparison between different turbulence models for boundary layer flows. He also examined alternatives to the no-slip boundary conditions. It turns out that constant eddy viscosity in combination with a partial slip conditions results in a good representation of the vertical flow structure and the shear stress at the bed level.

The partial slip condition at the bed ($z = h$) is given by:

$$\tau_b = A_v \frac{\partial u}{\partial z} = S u_b \tag{6}$$

where τ_b is the volumetric bed shear stress [m^2/s^2]. The slip parameter S determines the resistance at the bed; $S \to \infty$ would amount to a no slip condition.

Paarlberg et al. (2005) calibrated the values of A_v and S using flume measurements of the actual velocity profile and the bottom shear stress.

2.3 *Sediment transport model and bed behaviour*

Only bedload sediment transport is considered in the model, since this is assumed to be the main transport mechanism behind dune development. A general bed load formula including bed slope effects is applied:

$$q_b = \alpha |\tau_b|^\beta \left[\frac{\tau_b}{|\tau_b|} - \lambda \frac{\partial h}{\partial x} \right] \tag{7}$$

where q_b is the volumetric bed load transport [m^2 s^{-1}]. The proportionality constant α [s^2 m^{-1}] describes how efficiently the sand particles are transported by the bed shear stress (Van Rijn 1993) and strongly determines the time-scale of bed evolution. Parameter β represents the nonlinear dependence of sediment transport on the bed shear stress. The bed slope parameter λ describes the downhill preference of moving sediment.

Table 1. Parameter values for a model run where no flow separation occurs (Figure 1).

Par.	Description	Value	Dim.
A_v	eddy viscosity	$1.9 \cdot 10^{-4}$	m^2/s
S	slip parameter	$1.9 \cdot 10^{-3}$	m/s
g	acceleration of gravity	9.81	m/s^2
q	specific discharge	0.038	m^2/s
i	mean bottom slope	$5.5 \cdot 10^{-4}$	-
H	average water depth*	0.10	m
α	prop. constant	0.3	s^2/m
β	power of τ_b	1.5	-
λ	slope parameter	0.1	-

*: the average water depth may vary during a simulation, as a result of changing bed roughness.

Bed evolution follows from the Exner equation:

$$(1 - \epsilon_p) \frac{\partial h}{\partial t} = -\frac{\partial q_b}{\partial x} \tag{8}$$

where ϵ_p is bed porosity (typically $\epsilon_p \sim 0.4$).

2.4 *Results*

The model presented in this section cannot treat flow separation, since the pressure distribution is hydrostatic. However, the model should be able to reproduce the main characteristics of dune development in the case of streamlined flow (no flow separation). Figure 2 shows results of a simulation with an initially small symmetrical bed disturbance and periodic boundary conditions. Used parameter values are specified in Table 1 (see also Paarlberg et al. 2005).

The figure shows that over time the dunes grow in amplitude and migrate in streamwise direction. Further, it can be observed that dune asymmetry (ratio of

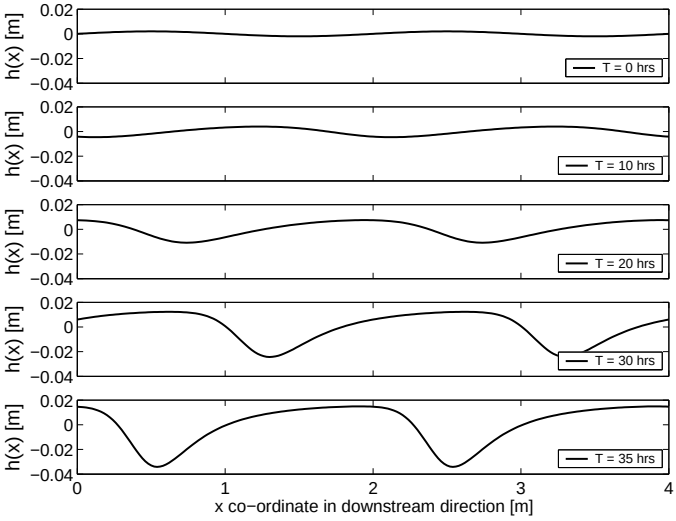

Figure 2. Development of small initial disturbance (2mm). See Table 1 for model parameter settings. Flow is from left to right. T are flow hours.

stoss- and lee-side slope) increases over time. These processes are well known processes in dune development, giving confidence in the used model equations. However, to enable determination of equilibrium dune dimensions the model needs to be extended to enable simulations in cases where flow separation occurs.

3 FLOW SEPARATION

3.1 *Process of flow separation*

Flow over a river bed is driven by gravity. Seen in vertical direction the pressure gradient is linear between the watersurface (zero) and the bed ($\rho g h_l i$, with h_l the local water depth) for parallel and non-curved streamlines. This condition holds more or less for slowly accelerating flow over the stoss side of a dune.

If we consider flow over a dune, such as shown in the bottom panel of Figure 2, the pressure gradient in horizontal direction is positive (or adverse) at the lee-side of the dunes due to an increasing local water depth. This adverse pressure gradient is most pronounced in the region close to the bed. Here momentum is lowest, leading to a velocity profile with a $\partial u/\partial z$ of zero near the bottom. Even further downstream on the lee-side, where the adverse pressure gradient is larger, reverse flow is observed. As a result of the reversed flow, a flow separation zone will form behind steep dunes. Here, the location where the flow separates is termed the flow separation point (FSP).

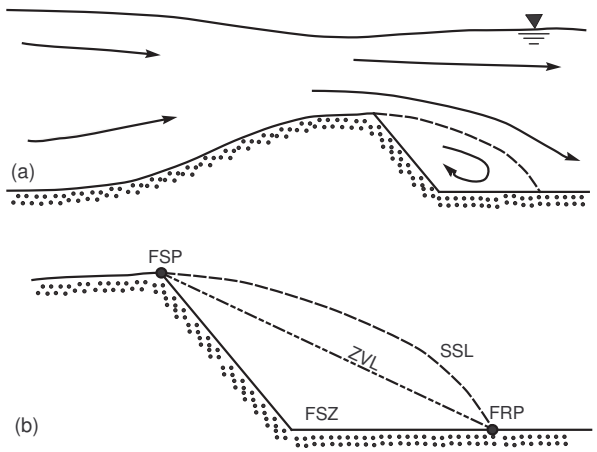

Figure 3. (a) streamlines and water surface profile over a typical dune shape (vertical exaggeration). (b) emphasis on the flow separation zone (abbreviations are explained and used in the text).

Figure 3 shows flow over a typical dune with presence of a flow separation zone (FSZ). The flow reattaches to the bed at a typical distance of about 6 times the dune height at the flow reattachment point (FRP). The separating streamline (SSL) indicates the boundary between the recirculating flow cell, and the normal flow field. The zero velocity line (ZVL) connects the points where the horizontal velocity is zero. The abbreviations used in this section are included in Figure 3 for later reference.

3.2 *Parameterization of the shape of the flow separation zone*

Paarlberg et al. (2005) propose a parameterization of the shape of the flow separation zone, based on the approach of Kroy et al. (2002). They state that formation and migration of aeolian sand dunes do not very sensitively depend on the details in the FSZ. Since there is flow recirculation in the FSZ, it is assumed that computation of the flow field above the separating streamline is sufficient. Therefore, a parameterization of this separating streamline was developed by Paarlberg et al. (2005).

The main concepts of the parameterization are:

- The shape of separation zone is independent of flow conditions;
- The SSL can be represented by a 3^{rd} order polynomial: $s(x) = s_3(x_*)^3 + s_2(x_*)^2 + s_1(x_*) + s_0$, with $x_* = x - x_s$ and x_s the position of the FSP;
- There is smooth connection at separation point giving s_1 and s_0;
- The (dimensionless) length of the separation zone can be estimated from (see Paarlberg et al. 2005 for determination of coefficients):

$$L_{fsz}/H_{dune} = 0.19\alpha_s + 5.66 \qquad (9)$$

  where L_{fsz} the FSZ-length, H_{dune} the dune height at separation and α_s the local bed slope at separation (degrees);
- The angle of the SSL at the FRP is -25° with the average bottom slope.

4 THE MORPHODYNAMIC MODEL

To include flow separation, the numerical model described in Section 2 is extended with the parameterization for flow separation as described in Section 3. Figure 4 shows a schematic representation of the morphodynamic model setup, which will be explained in this section. If there is no flow separation, the left part of Figure 4 is followed which is the model as described in Section 2. When flow separation does occur the model follows the right part in Figure 4.

4.1 *Flow separation criterion in the model*

In the flow solver, no pressure distributions are computed. The criterion for flow separation to occur is based on local bed gradients. Strong (negative) bed gradients result in an increase of adverse pressure gradient. In line with e.g. Kroy et al. (2002) we use the following separation criterion: separation occurs if the local bed gradient exceeds -14° (with the mean bottom slope).

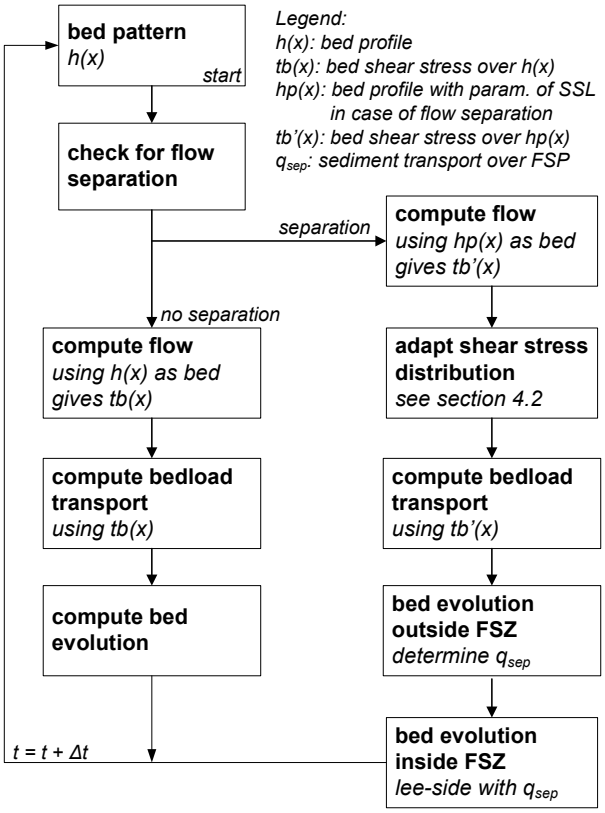

Figure 4. Schematic representation of the morphodynamic model.

4.2 *Bed shear stress distribution over a dune*

In our approach, flow is computed over the SSL above the FSZ, and over the bed elsewhere. Thus the flow inside the FSZ is not computed explicitly. Figure 5 shows an example of the bed shear stress distribution over two identical dunes with flow separation.

Measurements show that the time-averaged bed shear stress approximates zero in the FSZ (see e.g. Van Mierlo and De Ruiter 1988). Furthermore, if bedload transport is dominant, the sediment flux in the FSZ is close to zero due to flow recirculation in the FSZ. The flow computation over the parameterized bed ($hp(x)$) is used to give a first estimate of the bed shear stress distribution over the dunes. Next, the average bed shear stress (and thus the flux) is set to zero inside the FSZ. This procedure results in two discontinuities in the shear stress distribution over a dune. At the FSP the bed shear stress goes to zero. In Section 4.3 will be shown that this is no problem because of the method used for bed evolution inside the FSZ. However, the discontinutiy at the FRP must be resolved. Therefore, we need a parameterization for the distribution of the average bed shear stress over the stoss-side of the dunes.

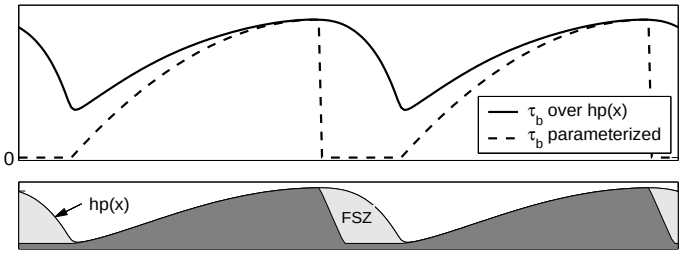

Figure 5. Parameterization of bed shear stress distribution over a dune. The bottom panel gives an arbitrary bed profile with flow separation zones (FSZ) indicted. The top panel gives the computed and parameterized bed shear stress distribution.

Table 2. Measurements that are used to obtain a bed shear stress distribution for the model. General dune and flow characteristics, used scaling parameters for Figure 6, and general flow characteristics are included.

	(a)	(b)	(c)	(d)
λ	0.6	0.39	1.6	1.6
Δ	0.03	0.03	0.08	0.08
L	0.51	0.25	1.16	1.16
τ_m	0.72	0.30	1.12	1.50*
i	$3.5 \cdot 10^{-4}$	$5.3 \cdot 10^{-4}$	$9.4 \cdot 10^{-4}$	$9.4 \cdot 10^{-4}$
H	0.200	0.130	0.290	0.372
q	0.070	0.037	0.099	0.171

λ: Dune length [m]; Δ: Dune height [m]; L: Distance between FRP and next crest position [m]; τ_m: Maximum bed shear stress [N/m^2] (the latter two parameters are used as scaling parameters in Figure 6); i: Average bottom slope [-]; H: Average water depth [m]; q: Specific discharge [m^2/s]; *: measured shear stress was slightly higher due to horizontal section just before top; (a): Vittal (1972); (b): Raudkivi (1963); (c,d): Van Mierlo and De Ruiter (1988).

Figure 6 shows measurements of (dimensionless) bed shear stress distributions over dunes (dune characteristics can be found in Table 2). At the FRP the measured time-averaged bed shear stress is zero, and downstream of the FRP the time-averaged bed shear stress gradually increases until it reaches a maximum at the dune crest. To mimic this behaviour a curve

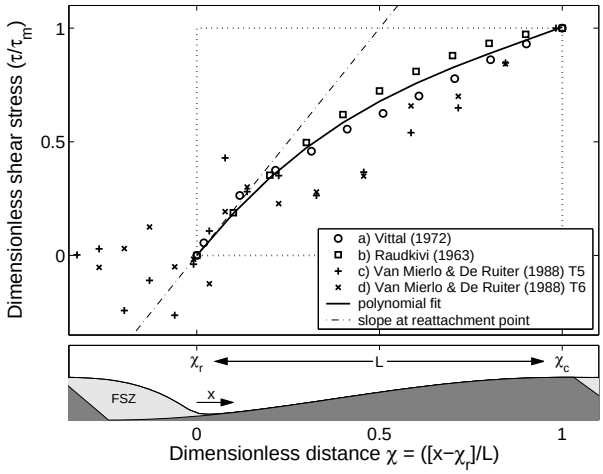

Figure 6. Measured bed shear stress distributions over dunes. For case (a) and (b) the data points are directly taken from reported literature; for case (c) and (d) the values are derived by assuming a logarithmic velocity profile close to the bed. The horizontal axis is scaled by $L = \chi_c - \chi_r$, being the horizontal length between the FRP and the next bedform top. The vertical axis is scaled by the maximum bed shear stress measured at the top (see also Table 2).

is fitted through these measurement points. Since we are interested in the shear stress on the stoss-side of a dune only measurements in the rectangular box in Figure 6 are used. The solid line in Figure 6 is a third order polynomial fit through the data, which fits quite well to the data. Therefore, we choose to approximate the bed shear stress distribution over a dune with a third order polynomial:

$$\tau'(\chi) = \begin{cases} 0 & \text{if } \chi < 0 \text{ (FSZ)} \\ a_3(\chi)^3 + a_2(\chi)^2 & \\ +a_1(\chi) + a_0 & \text{if } \chi_r \leq \chi \leq \chi_c \end{cases} \quad (10)$$

where χ is a dimensionless position along the dune (see Figure 6), and the coefficients $a_0 \ldots a_3$ are calibrated using the measurements. Parameter a_0 equals zero, since the bed shear stress is zero at the reattachment point (χ_r) and for a_1 holds at χ_r:

$$\left.\frac{d\tau'}{d\chi}\right|_{\chi_r} = 2\frac{\tau_m}{L}, \quad L = \chi_c - \chi_r \quad (11)$$

The coefficients a_2 and a_3 are calibrated by imposing smooth connection to the computed bed shear stress (and gradient in bed shear stress) at the crest of a dune.

4.3 *Bed evolution*

Bed evolution in the region outside the FSZ is determined by computing sediment transport and bed level changes by applying Eqs. (7) and (8). Since the time-averaged bed shear stress is set to zero inside the FSZ, there is no sediment transport in that zone. To schematize bed deformation in the FSZ, the material that passes the FSP is assumed to avalanche down the lee-side of the dunes and to be distributed evenly over the lee-side, with a lee-side angle at the angle of repose φ (for natural sand $\varphi \sim 30°$).

When performing this operation numerically, two small errors are made at each numerical timestep: 1) a "truncation error", being the difference between the volume that should be stored behind the dune and the amount that is actually stored; this error is kept within 1×10^{-6} m^2, and 2) a "rounding error" due to interpolation to the grid when the lee-side of the dune is set (this error is of order 1×10^{-5} m^2). The sum of both errors implies that either too few or too much sediment is stored at the lee-side of the dune. This error is computed and corrected in the next morphodynamic update.

As may be observed in Figure 2, using the flow separation criterion discussed in Section 4.1, the position where flow separation occurs for the first time in the model is somewhere halfway the lee-side of the dune. In the model, from this moment onward separation occurs at the crest of the dune, inducing avalanching of sediment over the top. This process occurs fast compared to the overall timescale of dune development (migration of about order 10 m/day, see e.g. Wijbenga and Van Nes 1986), and is illustrated in Figure 7. Effectively, it means that the lee-side does not deform from the moment that it reaches a slope at the angle of repose, and that the distance that the lee-side moves downstream is determined by the sediment volume over the separation point and the dune height.

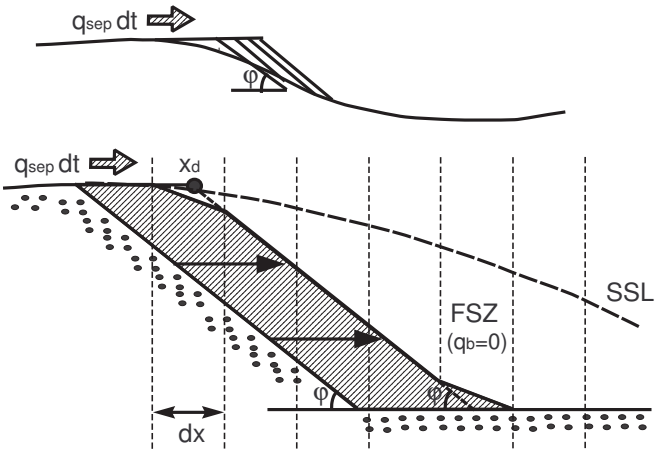

Figure 7. If flow separation occurs, a lee-side with an angle of repose (φ) is formed (top figure). The volumetric sediment transport ($q_{sep}dt$), where dt is the timestep, distributes evenly over the lee-side, as sketched in the lower figure. x_d is the horizontal position where the lee-side starts; dx is the horizontal grid distance. Due to interpolation to the grid in each time step, errors occur, which are compensated in the next time step.

5 RESULTS WITH FIXED DUNE LENGTH

In this section, the performance of the model from the previous section is presented. The eddy viscosity A_v and slip parameter S remain constant during the simu-

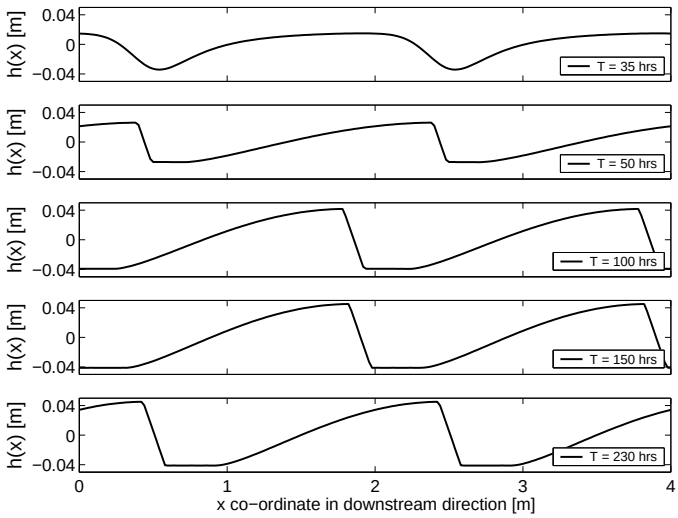

Figure 8. Long term development of two identical dunes. The top panel is the same as the last panel of Figure 2 with a different scale on the y-axis. T are flow hours.

lation. As bedforms develop over time, the roughness of the bed changes. Although the roughness (included in the model via the slip parameter S) is constant in a simulation, the average water depth H is changed to ensure a constant steady discharge. Simulations are made with periodic boundary conditions, putting restrictions on the wave length of simulated dunes (i.e. the dune length will remain constant).

5.1 *Bed evolution*

Simulations start with an initially flat bottom with very small disturbances. These disturbances develop into asymmetric features as shown in Section 2.4. Using the morphodynamic model discussed in the previous section, simulations can now be performed including the effect of flow separation. Parameter settings for the model runs presented here are the same as in Section 2.4. Figure 8 shows the long term evolution of two dunes, leading to typical dune shapes with a lee-side at the angle of repose.

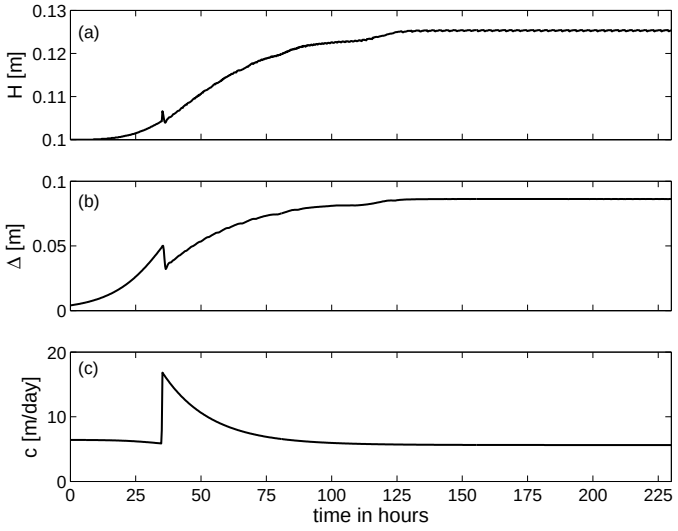

Figure 9. Development of average water depth H (a), dune height Δ (b), and migration velocity (c) over time for the simulation shown in Figure 8. The discontinuity is at the time where flow separation happens for the first time (after about 35 hours).

After sufficiently long time, a (dynamic) equilibrium is obtained as shown in Figure 9. The equilibrium is referred to as dynamic because the dunes still migrate in downstream direction, while their height remains constant. The dune height (defined as the vertical distance between crest- and trough elevation averaged over the two dunes) steadily increases, attaining an equilibrium height after about 130 flow hours. The average water depth (H) shows a similar behaviour, as a result of increasing flow resistance due to a growing FSZ.

Determination of the migration velocity of the dunes is not straightforward, because the dune profile deforms, as well. For example, in cases without flow separation, the crest of the dunes migrates faster than the trough. Since simulations initially start with a sinusoidal disturbance in a periodic domain, we choose to apply a fast fourier transform to determine the migration velocity of the Fourier mode most prominently present in the bed. The phase difference between the Fourier components at two subsequent timesteps is translated into an estimate of the migration velocity. Figure 9c shows, apart from the "discontinuity", that the migration velocity decreases with increasing dune height. Larger dunes, with constant dune length, imply lower migration velocities, since more sediment has to be moved.

The discontinuities in Figure 9 are related to our implementation of flow separation. The system suddenly switches from a situation without flow separation to one with flow separation. When this switch occurs, the system needs to adapt to the strong changes in bed shear stress distribution over the dunes. After about 35 flow hours, when flow separation occurs, the bed shear stress in the FSZ becomes zero and on the stoss side the bed shear stress gradient increases (i.e. Eq. (10)). From separation onwards, all the sediment transported over the FSP is stored in the FSZ behind the lee-side of a dune. This leads to a situation with a larger migration velocity, compared to a situation where the sediment was redistributed over a sinusoidal dune.

5.2 *Flow field and bed shear stress*

Figure 10 shows the bed velocity, the bed shear stress distribution and the velocity field in equilibrium after 150 flow hours. The dunes occupy a considerable height of the water column ($\Delta/H \approx 0.7$ in equilib-

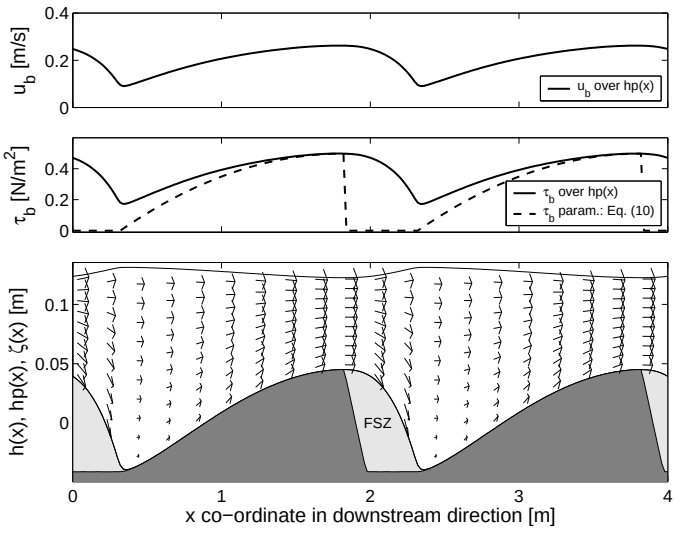

Figure 10. Bed velocity (top), bed shear stress (center) and velocity field (bottom) after 150 flow hours. Dark gray shading is the bed, light gray shade represents the FSZ, over which the flow is computed.

rium), and also water surface fluctuations are significant. The velocity at the bed increases over the stoss-side. Due to the partial slip condition, velocities near the bed differ from zero. Also we clearly see lower velocities at the bed compared to velocities at the surface.

5.3 *Comparison with measurements*

Between 1973 and 1980 a series of flume experiments with steady flow conditions and uniform sediment were carried out at the Delft Hydraulics Laboratory (Bakker et al. 1986). The measurements were performed in a flume which is 100 m in length and 1.5 m wide.

Figure 11 shows a series of recorded bed profiles for test T14 in equilibrium. The first 10 m of a 30 m long measurement section at the end of the flume are shown. In this experiment, which started with a bed profile resulting from a previous experiment, the following flow conditions hold in equilibrium: a specific discharge $q \approx 0.04$ m^2/s, an average water depth H = 0.106 m, and mean bottom slope $i = 1.06 \cdot 10^{-4}$. The energy slope is kept constant during the experiment by a weir at the downstream end of the flume. These conditions are comparable to the simulation that is performed. In the experiments, an equilibrium was attained after about 250 flow hours. In equilibrium, the average dune height is about 0.05 m, the average length about 1.7 m, and the migration rate is estimated at about 10 m/day. All these characteristics are in general agreement with our simulation, although the dune height seems somewhat over estimated by our simulation model. This may be due to our approximation

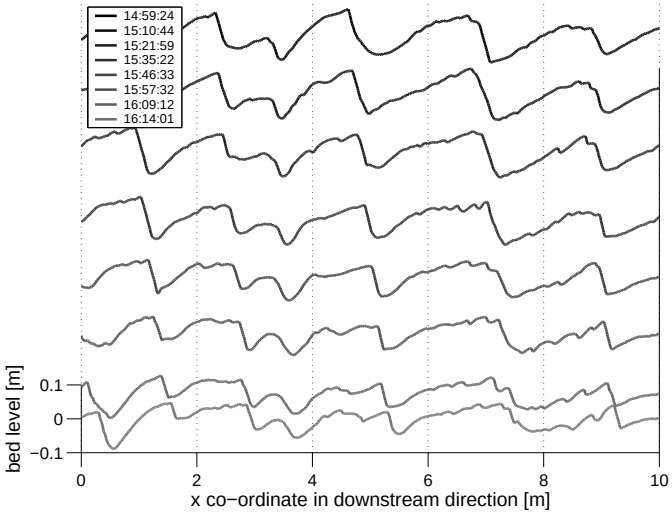

Figure 11. Bed profile measurements for TOW test T14 in equilibrium (Bakker et al. 1986). Test conditions: q = 0.04 m^2/s, H = 0.106 m, and $i = 1.06 \cdot 10^{-4}$. Time reads from top to bottom, and scale is indicated on the lower left side of the plot.

of constant eddy viscosity over depth, or the imposed constant dune length.

6 DISCUSSION

The proposed model is simple and fast in application, but highly parameterized. Some of the parameters maybe estimated a priori. An estimation of the eddy viscosity A_v can be obtained from a relationship that follows from integration of an parabolic eddy viscosity profile in vertical direction:

$$A_v = \frac{1}{6}\kappa u_* H \tag{12}$$

in which κ is the Von Kármán constant ($= 0.407$), and u_* is the shear velocity ($= \sqrt{gHi}$). Evaluating this equation for an initial water depth of $H = 10$ cm results in $A_v = 1.56 \times 10^{-4}$ m^2/s. This is very close to the calibrated value (see Table 1). The slip parameter S is more difficult to estimate, and may depend on grain-size, water depth and energy slope; for now, this remains a parameter for calibration.

The parameter α appearing in the sediment transport relationship is set to 0.3 following Van Rijn (1993). According to Komarova and Hulscher (2000) its value can be estimated with:

$$\alpha = \frac{m}{(s-1)g} \tag{13}$$

where s is the specific grain density ($= 1.65$), and m is an empirical coefficient, which may vary between 5.7 and 12 depending on the rate of sediment transport (Wiberg and Smith 1989). To arrive at a value of $\alpha = 0.3$, m should be about 5. Although this seems a quite low value, it is considered that the value of α primarily influences the rate of sediment transport and thus the timescale of bed evolution. It has only minor influence on the general bed behaviour.

In the proposed morphodynamic model, we do not account for turbulent fluctuations, and use the average bed shear stress to compute the sediment transport over the dunes. For sure we cannot reproduce all details of the complicated dune development process. However, our goal is to develop an appropriate model to reproduce general dune behaviour. Therefore, we believe that this approach is appropriate for our goals.

In the flow solver, no details of the turbulent flow inside the FSZ are computed. However, it is expected that there is an influence of the energy losses in the FSZ on the remainder of the flow field, since simulated water surface elevations above the FSZ are quite large. This influence is not included in the proposed model. It could be included by changing the boundary condition above the SSL (Eq. (6)) using a characteristic turbulent mixing length, e.g. the vertical distance between the ZVL and the SSL. This would require a depth-dependent eddy viscosity.

At the FRP the time-averaged bed shear stress is close to zero. However, experimental observations show that at the FRP much sediment is brought into transport. This is probably due to large fluctuations of the bed shear stress at the FRP. The influence could be included by imposing a fluctuation on the computed bed shear stress.

In our model, the dune length is assumed constant. However, e.g. Ten Brinke et al. (1999) observed that during dune development dunes do not only grow in amplitude, but their length also increases. Furthermore, a constant dune length has an influence on the model results, since a combination of dune height and dune length determines the steepness of the dunes (and thus influence the sediment transport via the slope parameter). Furthermore, a changing dune length is expected to be related to the influence of flow separation on equilibrium dune dimensions. Therefore, a next step in the model should certainly be to include a variable dune length in the model.

7 CONCLUSIONS

In this paper we present a morphodynamic model to simulate dune development. We focus on modelling processes that are most relevant to get a general idea of dune dimensions under certain flow conditions and sediment characteristics.

In cases where flow separation does not occur (i.e. when dunes have gentle slopes), the basis model qualitatively reproduces well known morphological behaviour: dunes grow in amplitude, migrate in streamwise direction, and become asymmetrical. These processes can be modelled using hydrostatic equations and a simple sediment transport model based on average bed shear stress.

Flow separation plays a key role in dune development. To keep the model appropriately, we follow an approach introduced by Kroy et al. (2002) to determine the shape of the flow separation zone on the basis of general dune dimensions (see also Paarlberg et al. 2005) and effectively cut off the flow separation zone from computations. The flow field is only computed above the flow separation zone and the sediment transport behaviour downstream of the reattachment point and in the flow separation zone, where no flow is computed, is parameterized. In the paper it is shown that the basis model, extended with this parameterization of flow separation is able to simulate dune development to equilibrium conditions, under steady discharge conditions. Moreover, the model is in general agreement with laboratory flume data.

Future work will focus on more detailed calibration and validation of the flow model, and the application of the model to unsteady flow conditions. Furthermore, the morphodynamic model will be extended to include variable dune length during the development process of dunes. When the model is applied to unsteady flood events, the dimensions of the dunes (length, height and steepness) and of the flow separation zone can be used to make predictions of the overall roughness that may be expected. This is very important for water manager to make accurate predictions of water levels.

8 ACKNOWLEDGEMENTS

This work is supported by the Technology Foundation STW, the applied science division of NWO and the technology programme of the Ministry of Economic Affairs (Project No. TCB.6222).

REFERENCES

Allen, J. R. L. (1976). Computational models for dune time-lag: general ideas, difficulties and early results. *Sedimentary Geology 15*, 1–53.

Bakker, B., A. J. Struijk, and H. Nijdam (1986, February). Flume experiments on dunes under steady flow conditions (uniform sand, d_m = 0.77 mm); description of bed forms, volume I-III. TOW rivers R 567 - XIX / M 1314 part VIII, WL | Delft Hydraulics, Delft, The Netherlands.

Fredsøe, J. (1979). Unsteady flow in straight alluvial streams: modification of individual dunes. *Journal of Fluid Mechanics 91, part 3*, 497–512.

Hulscher, S. J. M. H. (1996). Tidal-induced large-scale regular bed form patterns in a three-dimensional shallow water model. *Journal of Geophysical Research 101*, 20727–20744.

Julien, P. Y. and G. J. Klaassen (1995). Sand-dune geometry of large rivers during floods. *Journal of Hydraulic Engineering 121*(9), 657–663.

Julien, P. Y., G. J. Klaassen, W. B. M. Ten Brinke, and A. W. E. Wilbers (2002). Case Study: Bed resistance of Rhine River during 1998 flood. *Journal of Hydraulic Engineering 128*(12), 1042–1050.

Kennedy, J. F. (1969). The formation of sediment ripples, dunes and antidunes. *Ann. Rev. Fluid Mech. 1*, 147–168.

Komarova, N. L. and S. J. M. H. Hulscher (2000). Linear instability mechanics for sand wave formation. *J. of Fluid Mechanics 413*, 219–246.

Kroy, K., G. Sauermann, and H. J. Herrmann (2002). Minimal model for aeolian sand dunes. *Physical Review E 66*(3), 19 pp.

Nelson, J. M., A. R. Burman, Y. Shimizu, S. R. McLean, R. L. Shreve, and M. Schmeeckle (2005). Computing flow and sediment transport over bedforms. In G. Parker and M. H. Garcia (Eds.), *Proceedings of the 4^{th} IAHR Symposium on River, Coastal and Estuarine Morphodynamics, Urbana, Illinois, USA*, Volume 2, pp. 861–872. Taylor & Francis Group, London.

Németh, A. A. and S. J. M. H. Hulscher (2003). Finite amplitude sand waves in shallow seas. In *Proceedings 3rd Symposium on River, Coastal and Estuarine Morphodynamics*, Barcelona, Spain, pp. 435–444. IAHR.

Németh, A. A., S. J. M. H. Hulscher, and R. M. J. Van Damme (2006). Simulating offshore sand waves. *Coastal Engineering 53*, 265–275.

Onda, S. and T. Hosoda (2004). Numerical simulatin on development process of dunes and flow resistance. In

M. Greco, A. Carravetta, and R. Della Morte (Eds.), *Proceedings of River Flow 2004, Napoli, Italy*, Volume 1, pp. 245–252. Frederico II University of Napoli: Balkema publishers, Leiden, the Netherlands.

Paarlberg, A. J., C. M. Dohmen-Janssen, S. J. M. H. Hulscher, and A. P. P. Termes (2005). A parameterization of flow separation in a river dune development model. In G. Parker and M. H. Garcia (Eds.), *Proceedings of the 4^{th} River, Coastal and Estuarine Morphodynamics conference, Urbana, Illinois, USA*, Volume 2, pp. 883–895. Taylor & Francis Group, London.

Raudkivi, A. J. (1963). Study of sediment ripple formation. *Journal of the Hydraulics Division 89*(6), 15–33.

Soulsby, R. L. (1990). Tidal-current boundary layers. *In: The Sea, Vol. 9. Ocean Engineering Science, B. Le Mehaute and D. Hanes (eds.)*, 523–566.

Stansby, P. K. and J. G. Zhou (1998). Shallow water flow solver with non-hydrostatic pressure: 2D vertical plane problems. *International Journal of Numerical Methods in Fluids 28*, 541–563.

Ten Brinke, W. B. M., A. W. E. Wilbers, and C. Wesseling (1999). Dune growth, decay and migration rates during a large-magnitude flood at a sand and mixed sand-gravel bed in the Dutch Rhine river system. *Spec. Pub., Int. Assoc. Sediment. 28*, 15–32.

Van den Berg, J. and R. Van Damme (2005). Sand wave simulation on large domains. In G. Parker and M. H. Garcia (Eds.), *Proceedings of the 4^{th} conference on River, Coastal and Estuarine Morphodynamics, Urbana, Illinois, USA*, Volume 2, pp. 991–997. Taylor & Francis Group, London.

Van Mierlo, M. C. L. M. and J. C. C. De Ruiter (1988). Turbulence measurements above artificial dunes; Report on measurements. Report Q789, WL | Delft Hydraulics, Delft, The Netherlands.

Van Rijn, L. C. (1984). Sediment transport, part III: Bed froms and alluvial roughness. *Journal of Hydraulic Engineering 110*(12), 1733–1754.

Van Rijn, L. C. (1993). *Principles of sediment transport in rivers, estuaries and coastal seas*. AQUA Publications.

Vanoni, V. A. and L. S. Hwang (1967). Relation between bed forms and friction in streams. *Journal of the Hydraulic Division 93*, 121–144.

Vittal, N. (1972). Flow over triangular roughnesses in open channels. University of Roorkee, India.

Wiberg, P. L. and J. D. Smith (1989). Model for calculating bed load transport of sediment. *Journal of Hydraulic Engineering 115*(1), 101–123.

Wijbenga, J. H. A. and A. R. Van Nes (1986). Flow resistance and bedform dimensions for varying flow conditions; results of flume experiments with flood waves. TOW rivieren R 567 - XXV / M 1314 part XIII, WL | Delft Hydraulics, Delft, The Netherlands.

Wilbers, A. (2004). *The development and hydraulic roughness of river dunes*. Ph. D. thesis, University of Utrecht, Utrecht, The Netherlands.

Yoon, J. Y. and V. C. Patel (1996). Numerical model of turbulent flow over sand dune. *Journal of Hydraulic Engineering 122*(1), 10–18.